Liquid Crystals
Publication details, including instructions for authors and subscription information:
http://www.informaworld.com/smpp/title~content=t713926090

Electrohydrodynamic instabilities in chiral smectic C cells

J. A. M. M. Van Haaren[a]
[a] Philips Research Laboratories, Eindhoven, The Netherlands

To cite this Article Van Haaren, J. A. M. M.(1993) 'Electrohydrodynamic instabilities in chiral smectic C cells', Liquid Crystals, 14: 2, 297 — 306
To link to this Article: DOI: 10.1080/02678299308027644
URL: http://dx.doi.org/10.1080/02678299308027644

LIQUID CRYSTALS, 1993, VOL. 14, NO. 2, 297–306

Electrohydrodynamic instabilities in chiral smectic C cells

by J. A. M. M. VAN HAAREN
Philips Research Laboratories, P.O. Box 80000,
NL-5600 JA Eindhoven, The Netherlands

Experimental results are presented on the optical response of chiral smectic C cells of various thicknesses (between 2 and 9 μm) on AC voltages. For part of the voltage and frequency range the electric field induces patterns of disclination lines. The threshold voltages for these electrohydrodynamic instabilities turn out to be independent of the cell thickness for 4, 6, and 9 μm cell gaps. In the 2 μm cells, structural changes of the chiral smectic C texture are found at voltages below the threshold for the instabilities. The applicability of the Carr–Helfrich model for electrohydrodynamic instabilities in nematics to these chiral smectic C layers is discussed.

1. Introduction

The application of AC electric fields of various frequencies and amplitudes to liquid-crystalline systems has been studied for at least six decades [1]. In the late 1960s the study of more or less static instabilities caused by AC electric fields became driven by their potential application in so-called dynamic scattering mode displays [2]. Though today this type of effect is no longer used for display purposes [3], the electrohydrodynamic instabilities still receive a lot of attention, but now from a more fundamental type of interest: These systems turn out to be attractive to study non-equilibrium thermodynamic phenomena that give rise to the formation of spatial or temporal patterns [4, 5]. In the late 1960s Carr [6], Helfrich [7], and Dubois-Violette, de Gennes and Parodi [8] explained the occurrence of these electrohydrodynamic instabilities as a consequence of the anisotropy in the conductive and the dielectric properties of the nematic system (see also [4] and [9] for a review). Later on, these phenomena have been studied for smectic systems as well, starting with the smectic A and the smectic C phase [10–12]. The smectic layer structure gave rise to novel effects, but it also complicated their interpretation. The opportunity to find new phenomena and the difficulties in understanding them are even more apparent for the chiral smectic C phase [13, 14], as this phase is ferroelectric.

2. Experimental results

Experiments were performed on a number of test cells of various thicknesses (2, 4, 6 and 9 μm). The cells were made from glass substrates with a thin, conductive indium–tin oxide coverage. The alignment of the liquid crystal material was realized by using thin polyvinylalcohol layers, that were rubbed in a parallel way. The cells were filled with the mixture ZLI 3654 from E. Merck (Darmstadt, Germany), which has the following sequence of phases:

$$\mathrm{C}\ -30^{\circ}\mathrm{C}\ \mathrm{S}_{\mathrm{C}}^{*}\ 62^{\circ}\mathrm{C}\ \mathrm{S}_{\mathrm{A}}\ 76^{\circ}\mathrm{C}\ \mathrm{Ch}\ 86^{\circ}\mathrm{C}\ \mathrm{I}.$$

0267–8292/93 $10·00

Other relevant properties of the liquid crystal material are the dielectric constants at 25°C and 10 kHz driving voltage: $\varepsilon_\perp = 5{\cdot}6$ and $\varepsilon_\parallel = 3{\cdot}8$ and, also at 25°C, the spontaneous polarization $P_s = 26{\cdot}5\ \text{nC cm}^{-2}$ [15]. The cell spacing, which is defined by quartz spheres or chopped fibres, was checked by capacitance measurements on the filled cells. The data given in this work pertain to a series of four cells, one of each cell gap, that have been assembled, filled and used for experiments as a set. The observations have been verified qualitatively on a similar set of cells filled with the same liquid crystal material, which had been made previously for different purposes.

Following [16], a Cano–Grandjean wedge was used to measure the minimum cell gap at which the smectic helices are present: for this material this thickness is 21 μm, so the cells in the present experiments are too thin to allow the formation of a helical structure. In this respect the present experiment differs from the experiments in [13, 14]: they report results on thick cells with domains of mutually anti-parallel polarization directions, which are separated by dechiralization lines. ([13] reports on observations on a focal conic texture, whereas [14] gives results on cells that have a homogeneous director pattern, apart from the domains with anti-parallel polarization.) Although in the present experiment the director patterns are uniform in the lateral directions, they are not uniform throughout the thickness of the cell: in all cells, the presence of splayed director states is indicated by the absence of any orientation for the cells between crossed polarizers that gives extinction [17]. The specific resistivity of the liquid crystal in the cells was measured with a Sawyer–Tower circuit using a 50 Hz triangular wave voltage of 10 V amplitude. The resistivity that is measured in this way is some average of the parallel and perpendicular components of the resistivity tensor. The weighting function in this average is determined by the director pattern in the cell, which is not known in detail. As the difference between the conductive properties parallel and perpendicular to the director is estimated to be relatively small (typically 20 per cent) [13] no efforts have been made to specify this weighting function. I found an average value for the resistivity equal to $3{\cdot}1 \times 10^8\ \Omega\text{m}$ at 25°C. Combining the charge conservation equation and Ohm's law, both for an isotropic liquid, gives a characteristic frequency, up to which ionic charges are able to follow an AC electric field [4, 13, 14], that equals $(2\pi\rho\varepsilon\varepsilon_0)^{-1}$. Using for ε an averaged value of the dielectric permittivity, this characteristic frequency equals 12 Hz for the present cells at 25°C.

Sinusoidal voltages are applied to the cells with effective values up to 50 V and frequencies up to 40 kHz. (Throughout this paper the AC voltages are sines and their strengths are specified by their effective values.) The electro-optic response is observed with a polarized light microscope (Leitz Aristomet) in transmission.

Four different ranges of electro-optical responses are discerned: depending both on the amplitude and the frequency of the applied voltage. For voltages with an effective value of typically 20 V, the following frequency ranges may be identified: At low frequencies (up to about 50 Hz) remanent texture changes are observed. At high frequencies (above 10 kHz) the cells are found to switch between laterally uniform states. At intermediate frequencies two types of patterns of disclination lines are found, one at relatively low frequencies (between about 50 and 500 Hz) and the other one at higher frequencies (up to about 10 kHz).

At voltages below the thresholds for the onset of the two types of instabilities, the cell's interference colours are noted to change in response to variation of the amplitude of the applied voltage. Figure 1 shows interference colours observed from a 4 μm cell driven by a 15 kHz, 23 V AC voltage. The cell contains different domains with different

colours and, consequently, with different director states. The white areas in this 4 μm cell remain white while rotating the cell between crossed polarizers. They do not occur in the 6 and 9 μm cells. Figure 2 shows an example of disclination lines at a lower frequency. These instabilities show a net growth along the rubbing directions. This agrees well with the observations in [11] and [12] for the (non-chiral) smectic C phase. The pattern formed by these lines is not a very regular one, and the disclination lines are not as sharp as those observed at higher frequencies. Knowing the orientation of the chiral smectic C chevron in and outside zig-zag defects [18], I found that the low frequency defect lines grow in the direction pointed at by the chevron tip. Examples of the instabilities that emerge at higher frequencies are shown in figures 3 and 4. These pictures have been taken for the 6 μm cell, but similar patterns are observed in the cells with 4 and 9 μm gaps. These instabilities are visible as periodic patterns of disclination lines that appear sharper and more regular than the ones at lower frequencies. The typical lateral periodicity of the lines in these cells is 4 μm, as is derived from the distance between diffraction spots observed when illuminating the pattern of disclination lines with a He–Ne laser. The lines are observed in two directions with a 45° angle between them (see figure 3). The rubbing direction bisects the obtuse angle between these two directions. We could interpret the directions in the following way: The two types of stripes run perpendicularly to the two directions that are at an angle of $\pm\theta$ with the rubbing direction, where θ is the chiral smectic C tilt angle. (For the present material ZLI 3654 θ equals 24·5° at 25°C and 21·5° at 45°C [15].) From the observations that the cells do not yield extinction between crossed polarizers, we know that it is not correct to identify these $\pm\theta$ directions with the orientation of the director pattern in the cell. However, if we were to make this identification, the directions for the stripes are in accordance with the ones in [11, 12]. This difficulty in interpretation of the direction of the stripes may be solved by stating that the direction of the stripes is determined by a part of the layer in the cell with a 22·5° angle between the rubbing direction and the director. Figure 3 shows that the two directions for the instabilities may occur in a single domain in the cell, but figure 4 gives an example of two different domains with in each domain one direction for the instabilities.

By varying the height of the microscope stage, it is possible to focus on different disclination lines. As has been explained by Penz [19], this is a consequence of the formation of different director configurations in different parts of the cell in such a way that adjacent parts of the cell act as positive and negative lenses. The differences in height were measured to be 41 μm for the 9 μm cell (with an applied voltage of 500 Hz and 7·3 V effective value). Features in the liquid crystal layer (like the spacers) are in focus at an intermediate height of the stage. Both patterns of disclination lines are more or less static: though driven by AC voltages with a relatively short period time, the defect lines are observed to grow in a steady (DC) way. For voltages just above the threshold, the ends of the defect lines propagate slowly through the cell (typically 10 μm s^{-1}, in agreement with results in [13]). In this way the density of defect lines increases with time during which the voltage is applied to the cell. The lines running at an oblique direction to the rubbing direction are visible over a large temperature interval in the chiral smectic C phase. Upon increasing the temperature, they disappear at 56°C, which is 6°C below the chiral smectic C to smectic A transition for the material under consideration. However, it must be noted that the temperature of the liquid crystal layer will be higher than the temperature of the cell's environment, because of the dissipation of the AC currents through the indium–tin oxide films at the inside of the cell.

Figure 2

Figure 4

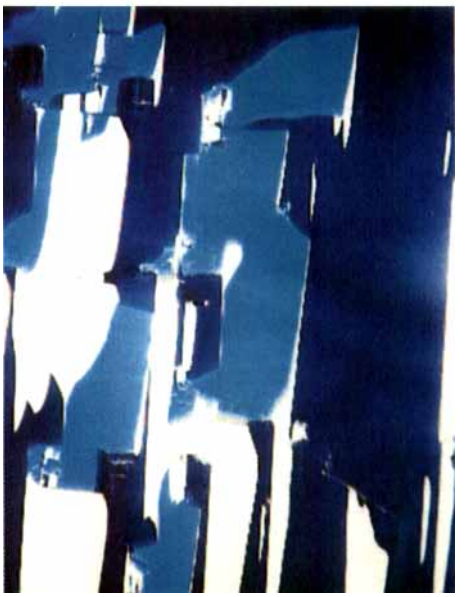

Figure 1

Figure 3

The effective value of the threshold voltage for the onset of the instabilities as a function of the frequency, measured at 25°C, is given in figure 5 for the cell with 9 μm thickness. At frequencies above 2 kHz, the threshold voltage in the thicker cells increases approximately linearly with the applied frequency. Figure 6 shows the results for four cells with different thicknesses. The threshold for the onset of the instabilities in the 4, 6, and 9 μm cell occurs at a threshold voltage that depends on the frequency, but not on the cell thickness. In the 2 μm cells, however, a structural change of the chiral smectic C texture [20–23] is found at voltages below that threshold value. The values at which this texture change occurs in the 2 μm cell are depicted in figure 6. The measuring voltages do not cause structural damage to the 4, 6 and 9 μm layers, although in the 4 μm cell texture changes could be induced with a 17 V, 800 Hz voltage, applied for several minutes, which is far beyond the threshold for the instabilities. The response to variation of the amplitude of the applied AC voltage is notably delayed, which is indicative of ionic effects.

To study the influence of the ionic effects in more detail, I measured the threshold voltages as a function of frequency on the same cells at 45°C (see figure 7). At this temperature P_s is 16·1 nC cm^{-2} [15] and the specific resistivity of the liquid crystal was measured to be $1{\cdot}2 \times 10^8\ \Omega$m, and the characteristic frequency $(2\pi\rho\varepsilon\varepsilon_0)^{-1}$ is equal to about 30 Hz. The threshold voltage versus frequency curves at 45°C have been shifted towards higher frequencies as compared to the ones at 25°C. Again, the applied voltages do not cause structural damage to the thicker layers, and the response to variation of the applied voltage is notably retarded.

A photomultiplier was used to monitor the optical response on a millisecond time-scale for a 10 kHz driving voltage. A periodically varying transmission with frequency equal to that one of the driving voltage is found. This response is also observed for amplitudes that are too small to generate a pattern of instability lines. A phase difference between the optical response and the applied voltage is observed, equal to about 90°, for frequencies between 5 and 30 kHz. At higher frequencies the phase difference between the optical response and the voltage decreases. At 70 kHz the optical response is in phase with the applied voltage, and the modulation depth at 8 V applied voltage has become small (3 per cent). In this respect, it must be noted that the series

Figure 1. Picture of a 4 μm cell at 25°C under application of a 15 kHz AC voltage at 23 V effective value. The displayed area of the cell is 800 μm × 640 μm. The cell is viewed between crossed polarizers. The rubbing direction is about parallel to the vertical boundary of the picture and points downwards.

Figure 2. Picture of a 6 μm cell at 25°C between crossed polarizers, under application of a 500 Hz AC voltage at 10 V effective value. The cell area that is shown in the picture is 400 μm × 320 μm. The rubbing direction is about parallel to the vertical boundary of the picture and points upwards.

Figure 3. Picture of a 6 μm cell at 25°C under application of a 800 Hz AC voltage at 10 V effective value. The shown area of the cell is 200 μm × 160 μm. The rubbing direction is about parallel to the vertical boundary of the picture and points upwards. The cell is viewed between crossed polarizers.

Figure 4. Picture of a 6 μm cell at 25°C under application of a 4 kHz AC voltage at 10 V effective value. The displayed area of the cell is 200 μm × 160 μm. The cell is viewed between crossed polarizers.

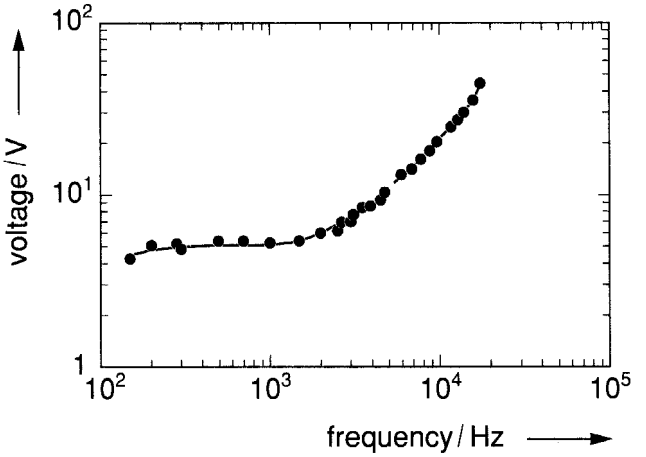

Figure 5. Effective value of the threshold voltage at which the instabilities emerge as a function of the frequency for the 9 μm thick cell at 25°C.

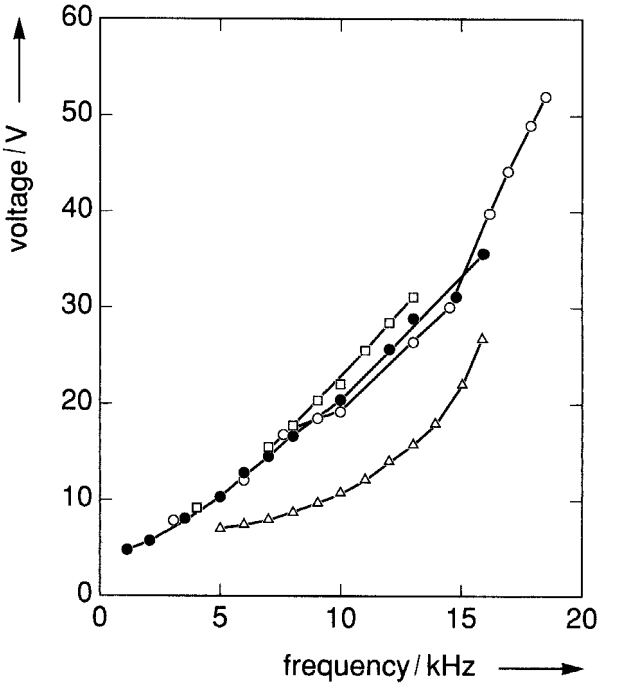

Figure 6. Effective value of the voltage for the onset of the instabilities as a function of the frequency for the 4 (□), 6 (○) and 9 μm (●) cells at 25°C. Some data points at the low frequency part of the graph have been left out, as they would coincide with the ones depicted for cells with another thickness. For the 2 μm (△) cell the instabilities are not observed, because relatively low voltage values cause a residual texture change (see text). For the 2 μm curve, the voltages at which this texture change is observed, are depicted. The data points for the 2 μm cell have been collected in order of increasing frequency.

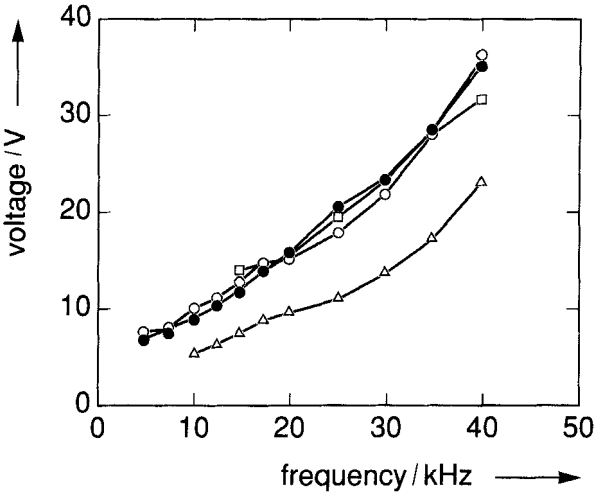

Figure 7. Effective value of the threshold voltage for the instabilities as a function of the frequency for the 4 (□), 6 (○) and 9 μm (●) cells at 45°C. For the 2 μm (△) cell the instabilities are not observed, because relatively low voltages cause a residual texture change (see text). The 2 μm curve gives the voltages at which this texture change is observed, while measuring these voltage data in order of increasing frequency.

circuiting of the resistance of the indium–tin oxide coating (which is less than 150 Ω in the present cells) and the capacitor formed by the liquid crystal layer (1·2 nF for the 2 μm cell) form an electronic low pass filter with corner frequency equal to 0·9 Mhz for the 2 μm cell and a larger one for the thicker cells. So the decrease of the modulation depth is not caused by filtering in the network formed by the indium–tin oxide, resistor and the liquid crystal capacitor.

3. Discussion

Before considering the electrohydrodynamic instabilities, it is worthwhile to discuss the colour changes and the optical response on a millisecond time-scale for driving voltages that are too small to give rise to the instabilities. For ferroelectric liquid crystals the electro-optical response may be interpreted in the following way: The electric field drives the director to one side of the smectic C cone, during the half-period in which the electric field has a positive polarity, and with an appropriate orientation of the cell between crossed polarizers this leads to an increase of the transmission. During the half-period in which the electric field has a negative polarity, the director is driven towards the opposite side of the cone, and the transmission decreases. For frequencies of about 10 kHz, the extreme values for the transmission turn out to occur at the sign-reversal of the driving voltage, thus yielding a 90° phase difference between the driving voltage and the optical response. This mechanism also provides an explanation for the colour changes upon application of the AC voltages: the voltages cause switching between different director profiles, each with their own interference colour. The perceived colours are a time-average of the colours that may be attributed to the various occurring director profiles. Upon increasing the amplitude, the director's sweep over the cone gets larger. At a certain amplitude, both extremal positions on the

smectic cone are reached, and further increase of the amplitude leads to a larger fraction of time in which the directors are in that extremal position, and consequently a larger contribution of the colours pertaining to these director states to the perceived colour of the cell. The white parts observed in the 4 μm cell (see figure 1) are caused by a mixing of complementary colours that happen to occur for this cell thickness. The presence of differently coloured domains in the cell over the entire voltage range studied, indicates that the cell contains areas with different director profiles. So driving the cell with an AC voltage with an amplitude just below the onset of the instabilities, the directors (and their associated net dipoles) are switching between two different splayed states at a frequency that equals the one of the driving voltage. The extremal states, between which the switching occurs, are different in different domains in the cell.

Upon further increase of the driving voltage, instabilities in the director pattern emerge. For nematics this phenomenon is well-understood. The instabilities that occur for driving frequencies well above $(2\pi\rho\varepsilon\varepsilon_0)^{-1}$ are explained by a model with fixed piled up charges and an oscillating director pattern [4, 6–9]. The starting point in this model, applied to materials with $\Delta\varepsilon \equiv \varepsilon_{\parallel} - \varepsilon_{\perp} < 0$, is that the electric field tends to keep the directors perpendicular to the electric field direction. The anisotropy in the conductive properties of liquid crystals is usually such that $\sigma_{\perp} < \sigma_{\parallel}$, and in that case an electric field applied normally to the liquid crystal layer gives rise to a lateral ionic current. The resulting local separation of charge leads to an additional electric field, which is directed in the plane of the liquid crystal layer. The directors tend to be perpendicular to the composite electric field, so they will be partially tilted and give rise to a bend distortion of the initially planar director pattern. Above a critical voltage, which may be argued to be independent of the sample thickness, the director pattern becomes unstable. The frequency and voltage range in which this mechanism is active is called the dielectric regime of electrohydrodynamic instabilities, as in this regime the charges are fixed and the director pattern and the associated dielectric tensor oscillate. In the case of ferroelectric liquid crystals, this model needs to be modified in four respects: In the first place, the polarization coupled to the director brings about a back-and-forth switching of the director in each period of the applied voltage, yielding different orientations for the director and the local polarization in the positive and negative part of the voltage wave-form. In non-ferroelectric liquid-crystalline media, there is no difference between the director orientations for positive or negative electric fields, as a sign-reversal of the electric field also generates a reversal of the direction of the induced polarization. Secondly, the torque that drives the director to a state perpendicular to the local electric field, is given by a coupling of the electric field $\boldsymbol{E}$ and both the induced polarization as well as the permanent one. As previously explained these torques have a different dependence on the azimuth-angle of the director on the smectic C cone. We may estimate that the ferroelectric torque due to the permanent polarization P_s has a maximum value as function of the director's azimuth angle equal to $P_s E$; for the dielectric torque this maximum is $\Delta\varepsilon\varepsilon_0 E^2(\sin\theta)^2/2$ (see [24], I assumed that the smectic layers are untilted). Using the parameters pertaining to the present material, both maximum torques are equal for $E = 190\ \mathrm{V}\ \mu\mathrm{m}^{-1}$. For smaller electric field strengths, such as the ones applied in the present experiment, the ferroelectric contribution to the torque exceeds the dielectric one. Consequently, the electric field should enter a model for instabilities in ferroelectric liquid crystals in a different power than in the non-ferroelectric case. In the third place, splay of the director pattern leads to space charge due to the divergence of the polarization, and we should calculate with the dielectric displacement rather than with the electric field. Fourthly, elastic properties for smectics

differ from those for nematics: as a consequence, the hydrodynamic flow occurs preferably inside the smectic planes [12].

The independence of the threshold voltage on cell thickness that is observed for the 4, 6 and 9 μm cells is also found for nematics. As for the frequency dependence, we may discern two frequency ranges: in the range up to about 1 kHz the threshold voltage was observed to be more or less constant, whereas for frequencies above 1 kHz the threshold voltage increases. Figure 5 shows that in the latter regime there is not a simple power law relation between the threshold voltage and the frequency: just above 1 kHz the threshold voltage may be considered to be linearly proportional to the square root of the frequency, and this dependence agrees both with the Carr–Helfrich description for nematics in the dielectric regime [4, 6 – 9], as well as with dielectric regime results on smectic C films [11] and on chiral smectic C films [13]. However, in the present experiment the frequency dependence of the threshold voltage was measured over a frequency range that is significantly larger than those in [11] and [13], and at higher frequencies a steeper increase of the threshold voltage is observed.

The nature of the disclination lines that occur at frequencies up to about 500 Hz (such as the one shown in figure 2) is not obvious. They are clearly different from the ones at higher frequencies (see figures 3 and 4). They resemble the co-called initial instabilities in the smectic C phase [11], which have been identified as instabilities in the conduction regime [12]. In this low frequency regime, the charges oscillate and generate a statically distorted director pattern. The observed independence of the threshold voltage with respect to frequency is consistent with literature results for this regime [4, 9, 11, 13]. However, the transition between the conduction and the dielectric regime is predicted to occur at the characteristic frequency $(2\pi\rho\varepsilon\varepsilon_0)^{-1}$ [4, 13, 14], and for the present cells $(2\pi\rho\varepsilon\varepsilon_0)^{-1}$ was calculated to be much smaller than 500 Hz.

4. Conclusion

It was observed that AC electric fields applied to chiral smectic C cells give rise to quasistatic patterns of instability lines. Two different types of instabilities could be discerned. The instabilities that occur for frequencies between 1 kHz and 20 kHz were interpreted as instabilities due to a piling up of ionic charges and an oscillating director pattern. The threshold voltage for these instabilities is a function of frequency. For cell gaps equal to 4, 6 and 9 μm, the threshold values do not depend on the cell thickness. The 2 μm cells show residual texture changes at voltages below the ones that give rise to the instabilities in the thicker cells. The second type of instabilities occur at frequencies below 500 Hz and are probably due to an oscillating ionic charge distribution and a static director profile. The Carr–Helfrich description of electrohydrodynamic instabilities in nematics was found to be helpful in the interpretation of the observations, but it does not incorporate the smectic geometry and the ferroelectricity of the material studied. In view of this, it is not surprising that part of the observations (the frequency dependence of the threshold voltages for the dielectric instabilities and the appearance of conductive instabilities at frequencies above $(2\pi\rho\varepsilon\varepsilon_0)^{-1}$) cannot be explained by this model.

I am indebted to J. I. M. Verbakel for preparing the test cells and to I. E. J. R. Heynderickx, C. J. E. Seppen and A. G. H. Verhulst for helpful discussions and critical reading of the manuscript.

References

[1] An early experimental study can be found in FRÉEDERICKSZ, V., and ZOLINA, V., 1933, *Trans. Faraday Soc.*, **29**, 919. For bibliographic references, see DURAND, G., 1976, *Les Houches Summer School of Theoretical Physics 1973* (Gordon & Breach), p. 403.

[2] HEILMEYER, G., ZANONI, L. A., and BARTON, L., 1968, *Proc. I.E.E.E.*, **56**, 1162.

[3] KANEKO, E., 1987, *Liquid Crystal TV Displays* (KTK Scientific Publishers), §2.2.

[4] DUBOIS-VIOLETTE, E., DURAND, G., GUYON, E., MANNEVILLE, P., and PIERANSKI, P., 1978, *Solid State Physics*, suppl. 14, edited by H. Ehrenreich, F. Seitz and D. Turnbull (Academic Press), p. 147.

[5] REHBERG, I., WINKLER, B. L., DE LA TORRE JUAREZ, M., RASENAT, S., and SCHÖPF, W., 1989, *Festkörperprobleme, Advances in Solid State Physics*, Vol. 29, edited by U. Rössler, (Vieweg), p. 35.

[6] CARR, E. F., 1969, *Molec. liq. Crystals*, **7**, 253.

[7] HELFRICH, W., 1969, *J. chem. Phys.*, **51**, 4092; 1970, *Ibid.*, **52**, 4318.

[8] DUBOIS-VIOLETTE, E., DE GENNES, P. G., and PARODI, O., 1971, *J. Phys., Paris*, **32**, 305.

[9] DE GENNES, P. G., 1975, *The Physics of Liquid Crystals*, second edition (Clarendon Press Oxford), §5.3.

[10] CHIRKOV, V. N., ALIEV, D. F., RADZHABOV, G. M., and ZEINALLY, A. Z., 1978, *Sov. Phys. J.E.T.P.*, **47**, 950.

[11] PETROFF, B., PETROV, M., SIMOVA, P., and ANGELOV, A., 1978, *Annls Phys.*, **3**, 331.

[12] PETROV, M., and DURAND, G., 1981, *J. Phys. Lett., Paris*, **42**, L519.

[13] LABROO, B., RAZDAN, V., PARMAR, D. S., and DURAND, G., 1985, *J. Phys. Lett., Paris*, **46**, L1177.

[14] JÁKLIV, A., BATA, L., and ÉBER, N., 1988, *Ferroelectrics*, **85**, 187; JÁKLIV, A., JÁNOSSY, I., and BATA, L., 1988, *Ferroelectrics*, **88**, 73.

[15] Data are given in: *Catalogue of Ferroelectric Smectic Mixtures* (E. Merck, Darmstadt, Germany), June 1989, unpublished.

[16] GLOGAROVÁ. M., LEJCEK, L., PAVEL, J., JANOVEC, V., and FOUSEK, J., 1983, *Molec. Crystals liq. Crystals*, **91**, 309.

[17] MACLENNAN, J. E., CLARK, N. A., HANDSCHY, M. A., and MEADOWS, M. R., 1990, *Liq. Crystals*, **7**, 753.

[18] CLARK, N. A., and RIEKER, T. P., 1988, *Phys. Rev.* A, **37**, 1053.

[19] PENZ, P. A., 1970, *Phys. Rev. Lett.*, **24**, 1405.

[20] DÜBAL, H.-R., ESCHER, C., and OHLENDORF, D., 1988, *Proceedings of the Sixth International Symposium on Electrets*, Oxford (I.E.E.E.), p. 344.

[21] SATO, Y., TANAKA, T., KOBAYASHI, H., AOKI, K., WATANABE, H., TAKESHITA, H., OUCHI, Y., TAKEZOE, H., and FUKUDA, A., 1989, *Jap. J. appl. Phys.*, **28**, L483.

[22] HARTMANN, W. J. A. M., and LUYCKX-SMOLDERS, A. M. M., 1990, *J. appl. Phys.*, **67**, 1253.

[23] VERHULST, A. G. H., and STOMMELS, F. J., 1991, *Ferroelectrics*, **121**, 79.

[24] XUE, JIU-ZHI, HANDSCHY, M. A., and CLARK, N. A., 1987, *Liq. Crystals*, **2**, 707.